Available online at www.sciencedirect.com
SCIENCE DIRECT®
Journal of Organometallic Chemistry 670 (2003) 198–204
Journal of Organometallic Chemistry
www.elsevier.com/locate/jorganchem

Reactions of metalloalkynes VII. Protonation of ruthenium ethyne-1,2-diyl complexes

Christopher S. Griffith [1], George A. Koutsantonis *, Brian W. Skelton, Allan H. White

Department of Chemistry, University of Western Australia, 35 Stirling Highway, Crawley, WA 6009, Australia

Received 12 November 2002; received in revised form 19 December 2002; accepted 19 December 2002

Abstract

The acid–base chemistry of some ruthenium ethyne-1,2-diyl complexes, $[\{Ru(CO)_2(\eta\text{-}C_5H_4R)\}_2(\mu_2\text{-}C{\equiv}C)]$ (R = H, Me) has been investigated. Initial protonation of $[\{Ru(CO)_2\{\eta\text{-}C_5H_4R\}\}_2(\mu_2\text{-}C{\equiv}C)]$ gave the unexpected complex cation, crystallised as the BF_4 salt, $[\{Ru(CO)_2(\eta\text{-}C_5H_4R\}\}_3(\mu_3\text{-}C{\equiv}C)][BF_4]$ (R = Me structurally characterised). This synthesis proved to be unreliable but subsequent, careful protonation experiments gave excellent yields of the protonated ethyne-1,2-diyl complexes, $[\{Ru(CO)_2\{\eta\text{-}C_5H_4R)\}_2(\mu_2\text{-}\eta^1{:}\eta^2\text{-}C{\equiv}CH)](BF_4)$ (R = Me structurally characterised) which could be deprotonated in high yield to return the starting ethyne-1,2-diyl complexes.

Keywords: Ruthenium; Ethyne-1,2-diyl; Protonation

1. Introduction

Much of the chemistry of metal alkynyl complexes is associated with their functional groups, namely the metal carbon bond and the electron density associated with the triple bond. Ethyne-1,2-diyl complexes constitute a special class of metal alkynyls whose chemistry is limited to a few examples. We have been investigating the chemistry of dimetalloalkynes or ethyne-1,2-diyl complexes [1–6] for some time now and have shown that they can exhibit a decidedly different reactivity to their monometallic relatives, particularly in our case where the 'piano-stool' geometry of the $\{Ru(CO)_2(\eta\text{-}C_5H_4R)\}$ substituent can perform various contortions to alleviate steric congestion unlike the more globular moieties such as $M(CO)_5$ (M = Re or Mn).

Bruce and co-workers [7,8] have provided the bulk of experimental support to the theoretical work of Kostic and Fenske [9] who calculated that the β-carbon atoms of metal alkynyls should be susceptible to attack by electrophiles. We were interested in the attack of simple electrophiles, such as the proton, on ethyne-1,2-diyls and how this would compare to the extant work in the analogous iron systems provided by Akita [10,11]. We report the results of these studies hereunder.

2. Experimental

2.1. General procedures

Manipulation of oxygen and moisture sensitive compounds was performed under an atmosphere of high purity argon using standard Schlenk techniques or in a dry box (Miller Howe).

Infrared spectra were recorded using a Bio-Rad FTS 45 or 40 FTIR spectrometer. ^{1}H- and ^{13}C-NMR spectra were acquired using Varian Gemini 200 or Bruker ARX 500 spectrometers. ^{1}H- and ^{13}C-NMR spectra were referenced with respect to incompletely deuterated solvent signals.

Mass spectra were obtained on a VG AutoSpec spectrometer employing a Fast Atom Bombardment (FAB) ionisation source in all samples unless otherwise specified. Elemental analyses were performed by the

* Corresponding author. Tel.: +61-8-9380-3177; fax: +61-8-9380-7247.
E-mail address: gak@chem.uwa.edu.au (G.A. Koutsantonis).
[1] Present address: Materials Division, Australian Nuclear Science and Technology Organisation (ANSTO) PMB 1, Menai, NSW 2234, Australia.

0022-328X/03/$ - see front matter © 2003 Elsevier Science B.V. All rights reserved.
doi:10.1016/S0022-328X(02)02196-4

Research School of Chemistry Microanalytical Unit, Australian National University, ACT.

Diethyl ether was dried over sodium metal and distilled from potassium benzophenone ketyl under an atmosphere of argon. Dichloromethane was dried over CaH_2 and distilled under an atmosphere of argon. Distilled ethereal solvents were stored over sodium or potassium mirrors until use.

The complexes $[RuCl(CO)_2(\eta\text{-}C_5H_5)]$, $[\{Ru(CO)_2(\eta\text{-}C_5H_4R)\}_2(\mu_2\text{-}C{\equiv}C)]$ (**1**) [12] and $[Ag_3(\{Ru(CO\}_2(\eta\text{-}C_5H_4R)\}_2(\mu_2\text{-}C{\equiv}C))_3](BF_4)_3$ [4], were prepared by the published procedures or modifications thereof.

2.2. Syntheses

2.2.1. Synthesis of $[\{Ru(CO)_2(\eta\text{-}C_5H_5)\}_3(\mu_3\text{-}C{\equiv}C)](BF_4)$ (**2a**)

To a solution of $[\{Ru(CO)_2(\eta\text{-}C_5H_5)\}_2(\mu_2\text{-}C{\equiv}C)]$ (**1a**) (30 mg, 0.064 mmol) in diethyl ether (20 ml) at ambient temperature, was added $HBF_4{\cdot}Oet_2$ (20 μl, 85% w/v solution) dropwise, giving an immediate yellow–orange precipitate. The supernatant was removed and the precipitate washed with diethyl ether (2×20 ml). Recrystallisation (CH_2Cl_2–Et_2O vap. diff.) yielded orange rods of **2a** (29 mg, 77%). Anal. Calc. for $C_{23}H_{15}B_1F_4O_6Ru_3$: C, 35.52; H, 1.94. Found: C, 35.63; H, 1.91%. IR (CH_2Cl_2): ν(CO) 2056m, 2049sh, 2003s cm^{-1}; ^{1}H-NMR (d_6-acetone) δ 5.80 (s, C_5H_5). ^{13}C-NMR(d_6-acetone) δ 206.0 (s, *C*O), 91.3 (s, C_5H_5). FABMS (NOBA–CH_2Cl_2) *m*/*z* 692 ($[M]^+$, 100%), 664–608 ($[M-(CO)_x]^+$ $x = 1$–3.

2.2.1.1. Alternative syntheses of ***2a****.* A mixture of $[Ru(CO)_2(\eta\text{-}C_5H_5)Cl]$ (**6**) (20 mg, 0.078 mmol) and $[Ag_3(\{Ru\{CO)_2(\eta\text{-}C_5H_5)\}_2(\mu_2\text{-}C{\equiv}C))_3](BF_4)_3$ (25 mg, 0.013 mmol) in methylene chloride (20 ml) was stirred at reflux (10 h). The cooled reaction mixture was then filtered through Celite and the volume reduced ca. 2 ml, with addition of diethyl ether (10 ml) giving an orange powder (18 mg, 85%) of the crude product. Subsequent recrystallisation (CH_2Cl_2–Et_2O vap. diff.) gave a sample with identical spectroscopic properties to that found for **2a**.

A mixture of $[Ru(CO)_2(\eta\text{-}C_5H_5)Cl]$ (**6**) (46 mg, 0.178 mmol), $[\{Ru(CO)_2(\eta\text{-}C_5H_5)\}_2(\mu_2\text{-}C{\equiv}C)]$ (**11a**) (50 mg, 0.107 mmol) and $[AgBF_4]$ (19 mg, 0.100 mmol) in methylene chloride (20 ml) was stirred for 48 h at ambient temperature. The reaction mixture was filtered through Celite and the volume reduced ca. 5 ml, with addition of diethyl ether (15 ml) giving an orange powder (35 mg, 45%) which exhibited identical spectroscopic properties to that found for **2a**.

2.2.2. Synthesis of $[\{Ru(CO)_2(\eta\text{-}C_5H_4Me)\}\{Ru(CO)_2(\eta\text{-}C_5H_4Me)\}_2(\mu_3\text{-}C{\equiv}C)](BF_4)$ (**2b**)

A mixture of $[RuCl(CO)_2(\eta\text{-}C_5H_4Me)]$ (26 mg, 0.096 mmol) and $[Ag_3(\{Ru(CO)_2(\eta\text{-}C_5H_4Me)\}_2(\mu_2\text{-}C{\equiv}C))_3](BF_4)_3$ (30 mg, 0.014 mmol) in dichloromethane (10 ml) was stirred at reflux (10 h). The cooled reaction mixture was then filtered through Celite and the volume reduced to ca. 2 ml, with addition of diethyl ether (10 ml) giving a pale orange powder of **2b** (33 mg, 95%). Anal. Calc. for $C_{26}H_{21}B_1F_4O_6Ru_3$: C, 38.09; H, 2.58. Found: C, 37.81; H, 2.46%. IR (CH_2Cl_2) ν(CO) 2054m, 2042m, 1992s cm^{-1}; ^{1}H-NMR (d_6-acetone) δ 5.70 (vt, 4H, C_5H_4Me), 5.61 (vt, 2H, C_5H_4Me), 2.09 (s, 12H, C_5H_4Me); ^{13}C-NMR (d_6-acetone) δ 200.1 (s, *C*O), 114.9 (s, C_i), 90.1 (s, C_5H_4Me), 88.2 (s, C_5H_4Me), 13.7 (s, C_5H_4Me); FABMS (NOBA–CH_2Cl_2) *m*/*z* 734 ($[M]^+$, 100%), 707–650 ($[M-(CO)_x(BF_4)]^+$ $x = 1$–3, 497 ($[M-(Ru(CO)_2(C_5H_4Me)(BF_4))]^+$, 6%).

2.2.3. Synthesis of $[\{Ru(CO)_2(\eta\text{-}C_5H_5)\}\{Ru(CO)_2(\eta\text{-}C_5H_4Me)\}_2(\mu_3\text{-}C{\equiv}C)](BF_4)$ (**2c**)

A mixture of $[RuCl(CO)_2(\eta\text{-}C_5H_5)]$ (23 mg, 0.090 mmol) and $[Ag_3(\{Ru(CO)_2(\eta\text{-}C_5H_4Me)\}_2(\mu_2\text{-}C{\equiv}C))_3](BF_4)_3$ (30 mg, 0.014 mmol) in dichloromethane (10 ml) was stirred at reflux (10 h). The cooled reaction mixture was then filtered through Celite and the volume reduced to ca. 2 ml, with addition of diethyl ether (10 ml) giving an orange powder of **2c** (31 mg, 90%). Anal. Calc. for $C_{25}H_{19}B_1F_4O_6Ru_3$: C, 37.27; H, 2.38. Found: C, 36.78; H, 2.25%. IR (CH_2Cl_2) ν(CO) 2055s, 2042m, 2001s cm^{-1}. ^{1}H-NMR (d_6-acetone) δ 5.81 (s, 5H, C_5H_5), 5.70 (vt, 4H, C_5H_4Me), 5.60 (vt, 4H, C_5H_4Me), 2.06 (s, 6H, C_5H_4Me). ^{13}C-NMR (d_6-acetone) δ 200.1 (s, *C*O{Ru(η-C_5H_4Me)}), 199.6 (s, *C*O, {Ru$(CO)_2(\eta$-$C_5H_5)$}), 115.5 (s, C_i), 90.7 (s, C_5H_4Me), 89.9 (s, C_5H_4Me), 88.2 (s, C_5H_5), 13.7 (s, C_5H_4Me). FABMS (NOBA–CH_2Cl_2) *m*/*z* 721 ($[M]^+$, 100%), 693–635 ($[M-(CO)_x]^+$ $x = 1$–3).

Complexes **2b** and **2c** can also be obtained in manner analogous to that described in Section 2.2.1.1 (second paragraph).

2.2.4. Synthesis of $[\{Ru(CO)_2(\eta\text{-}C_5H_5)\}_2(\mu_2\text{-}\eta^2\text{:}\eta^2\text{-}C{\equiv}CH)](BF_4)$ (**3a**)

To a stirred solution of $[\{Ru(CO)_2(\eta\text{-}C_5H_5)\}_2(\mu_2\text{-}C{\equiv}C)]$ (**1a**) (80 mg, 0.171 mmol) in diethyl ether (20 ml) at 0 °C was added $HBF_4{\cdot}Et_2O$ (50 μl, 85% w/v solution) dropwise, giving an immediate yellow precipitate. The reaction mixture was allowed to return to ambient temperature, then the colourless supernatant removed and the precipitate washed with diethyl ether (2×15 ml). Recrystallisation (CH_2Cl_2–Et_2O vap. diff.) yielded yellow rods of **3a** (85 mg, 89%). Anal. Calc. for $C_{16}H_{11}B_1F_4O_4Ru_2$: C, 34.54; H, 1.99. Found: C, 34.45; H, 2.04%. IR (CH_2Cl_2) ν(CO) 2072s, 2062s, 2018s

cm^{-1}; ^{1}H-NMR (CD_2Cl_2) δ 5.67 (s, 5H, C_5H_5), 3.86 (s, 1H, C≡C*H*). ^{13}C-NMR (CD_2Cl_2) 196.2 (s, *C*O), 90.3 (s, C_5H_5), 88.8 (s, *C*≡CH), 75.9 (brs, C≡*C*H); FABMS (NOBA–CH_2Cl_2) *m/z* 470 ($[M]^+$, 61%), 443–387 ($[M-(CO)_x]^+$ $x = 1$–3).

2.2.5. Synthesis of [{Ru(CO)$_2$(η-C$_5$H$_4$Me)}$_2$(μ$_2$-η^1:η^2-C≡CH)](BF$_4$) (3b)

To a stirred solution of [{Ru(CO)$_2$(η-C$_5$H$_4$Me)}$_2$(μ$_2$-C≡C)] (**1b**) (30 mg, 0.064 mmol) in diethyl ether (20 ml) at ambient temperature, was added $HBF_4 \cdot Et_2O$ (20 ml, 85% w/v solution) dropwise, giving an immediate yellow precipitate. The reaction mixture was stirred for 15 min then the pale yellow supernatant removed and the precipitate washed with diethyl ether (2×20 ml). Recrystallisation (CH_2Cl_2–Et_2O vap. diff.) yielded yellow rods of **3b** (29 mg, 77%). Anal. Calc. for $C_{18}H_{15}B_1F_4O_4Ru_2$: C, 36.99; H, 2.59. Found: C, 37.05; H, 2.76%. IR (CH_2Cl_2) *ν*(CO) 2074s, 2062s, 2020s cm^{-1}; ^{1}H-NMR (CD_2Cl_2) δ 5.02 (vt, 4H, C_5H_4Me), 4.96 (vt, 4H, C_5H_4Me), 3.83 (s, 1H, C≡C*H*), 1.57 (s, 6H, C_5H_4*Me*). ^{13}C-NMR (CD_2Cl_2) δ 196.9 (s, *C*O), 115.8 (s, C_i), 88.5 (s, C_5H_4Me), 87.0 (s, C_5H_4Me), 89.4 (s, *C*≡CH), 80.0 (brs, C≡*C*H), 13.1 (s, C_5H_4*Me*); FABMS (NOBA–CH_2Cl_2) *m/z* 499 ($[M]^+$, 100%), 470–414 ($[M-(CO)_x]^+$ $x = 1$–3).

2.3. Reaction of [{Ru(CO)$_2$(η-C$_5$H$_5$)}$_2$(μ$_2$-η^1:η^2-C≡CH)](BF$_4$) (3a) and NEt$_3$

To a solution of [{Ru(CO)$_2$(η-C$_5$H$_5$)}$_2$(μ$_2$-η^1:η^2-C≡CH)](BF$_4$) (**3a**) (25 mg, 0.045 mmol) in tetrahydrofuran (10 mmol) was added NEt_3 (0.5 ml, 3.96 mmol) and stirred for 10 h at ambient temperature. The solvent was removed in vacuo and the yellow residues extracted with toluene (30 ml). The volume of the solution was reduced ca. 20 ml and hexanes added to yield a pale yellow powder of **3a** (19 mg, 91%) which exhibited spectroscopic properties identical to an authentic sample.

2.4. Structure determinations of 2b and 3b

2.4.1. Experimental details

For **2b**, a full sphere of CCD area-detector data was measured (Bruker AXS instrument; $T \sim 300$ K; monochromatic Mo–K_α radiation; $\lambda = 0.71073$ Å; ω-scans, $2\theta_{max} = 50°$) yielding 15 771 reflections, merging to 4927 unique ($R_{int} = 0.027$) after 'empirical'/multiscan absorption correction (proprietary software), 3214 with $F > 4 < \sigma(F)$ considered 'observed'. For **3b**, a full sphere of single counter diffractometer data was measured at $T \sim 295$ K ($2\theta/\theta$ scan mode, $2\theta_{max} = 60°$), yielding 11 943 total reflections merging to 6015 unique ($R_{int} = 0.060$) after gaussian absorption correction, 3728 of these with $I > 3\sigma(I)$ considered 'observed' and used in the full-matrix least-squares refinement. Anisotropic displacement parameter forms were refined for the non-hydrogen atoms, (x, y, z, $U_{iso})_H$ being constrained at estimated values (both structures). Conventional residuals R, R_w (weights: $(\sigma^2(F) + 0.0004F^2)^{-1}$) on $|F|$ are quoted at convergence; neutral atom complex scattering factors were employed, computation using the XTAL3.5 program system [13]. Pertinent results are given below in Fig. 1 and Tables 1 and 2, the latter showing 20% (**3b**), 50% (**2b**) probability amplitude displacement envelopes for the non-hydrogen atoms, the hydrogen atoms having arbitrary radii of 0.1 Å.

In **3b**, the two BF_4^- groups were modelled as disordered about crystallographic inversion centres as trigonal bipyramidal envelopes with half weighted axial sites. The alkynyl hydrogen atom was located in a difference map.

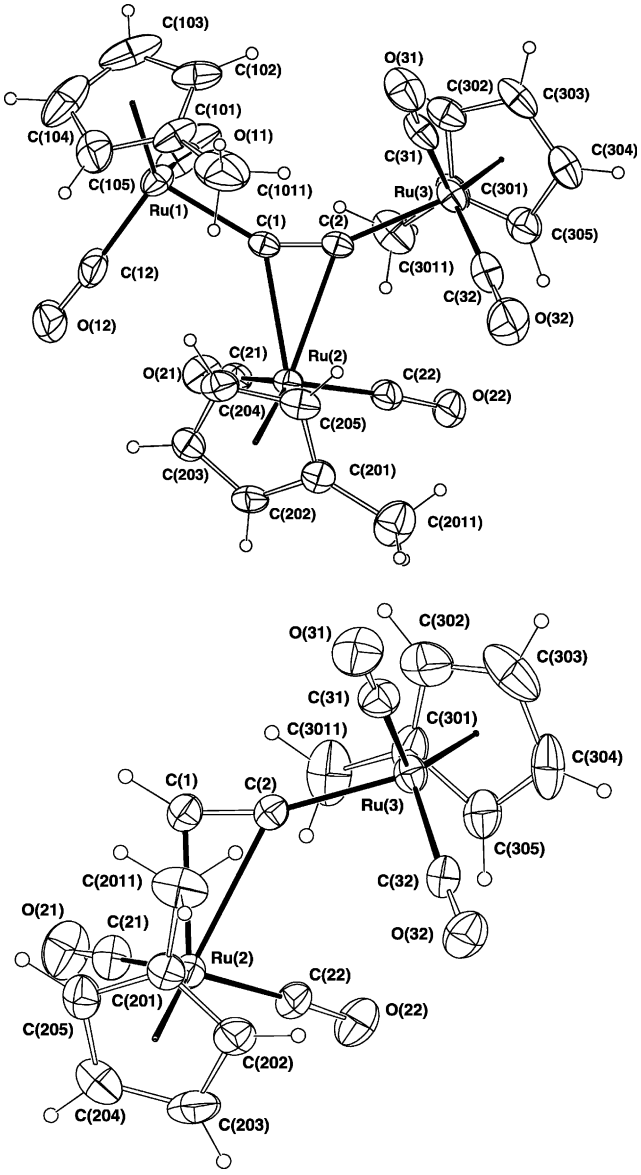

Fig. 1. Projections of **3b** (top), **2b** (bottom) normal to their Ru_2C planes.

Table 1
Comparative cation geometries

Compound	**2a**	**2b**	**2a**	**2b**	**3b**	**2a**	**2b**	**3b**
n	1		2			3		
Bond lengths (Å)								
Ru(n)–C(α)	2.065(6)	2.07(1)	2.044(6)	2.06(1)	2.023(5)	2.388(5)*	2.32(1)*	2.224(7)*
Ru(n)–C(n)	1.865(5)	1.85(1)	1.869(8)	1.85(1)	1.863(8)	1.878(6)	1.87(1)	1.885(6)
Ru(n)–C(n2)	1.860(6)	1.86(2)	1.880(7)	1.83(1)	1.893(7)	1.864(9)	1.86(1)	1.867(8)
C(n1)–O(n1)	1.147(7)	1.13(2)	1.13(1)	1.15(2)	1.14(1)	1.138(7)	1.14(1)	1.133(8)
C(n2)–O(n2)	1.136(9)	1.16(2)	1.13(1)	1.16(2)	1.112(9)	1.15(1)	1.16(2)	1.153(10)
Ru(n)–C(n00)	1–896	1.900	1.898	1.892	1.891	1.895	1.887	1.886
Ru(n)–C(n01–5)	2.216(6)	2.22(1)	2.228(7)	2.21(1)	2.19(1)	2.21(1)	2.20(1)	2.190(9)
	−2.258(5)	−2.25(2)	−2.25(1)	−2.28(1)	−2.26(1)	−2.243(8)	−2.25(1)	−2.283(7)
Average	2.24(2)	2.23(1)	2.238(9)	2.24(3)	2.23(3)	2.23(1)	2.23(2)	2.23(4)
Bond angles (°)								
C(α)–Ru(n)–C(n1)	87.7(3)	86.4(6)	86.4(3)	88.3(5)	86.8(3)	82.7(2)*	83.4(4)*	83.7(3)
C(α)–Ru(n)–C(n2)	95.6(3)	95.1(5)	92.6(3)	91.0(6)	92.8(3)	105.8(3)*	105.5(5)*	104.1(3)
C(α)–Ru(n)–C(n00)	121.0	121.8	122.1	122.2	121.5	116.6*	117.8*	119.0*
C(n1)–Ru(n)–C(n2)	90.2(3)	90.0(6)	91.3(3)	89.4(6)	91.0(3)	90.2(3)	90.2(5)	90.1(3)
C(n1)–Ru(n)–C(n00)	127.2	127.1	124.6	125.3	126.2	128.6	126.3	125.2
C(n2)–Ru(n)–C(n00)	124.7	125.6	128.4	128.9	127.3	123.9	124.3	124.9
Ru(n)–C(n1)–O(n1)	178.4(7)	179(1)	177.1(6)	178(1)	178.5(6)	175.6(6)	179(1)	179.3(7)
Ru(n)–C(n2)–O(n2)	176.1(6)	176(1)	179.7(8)	179(1)	177.1(6)	176.4(7)	176(1)	177.0(6)
Ru(n)–C(α)–C(β)	152.5(4)	149.3(8)	155.2(5)	156.7(8)	164.7(5)	77.9(4)	79.9(7)	88.7(5)
Ru(2)–C(α)–Ru(n)	129.5(3)	130.8(5)	132.7(3)	130.8(5)	132.7(3)	72.1(3) [a]	70.4(6) [a]	62.4(4) [b]

C(α) is that of C(1, 2) nearer the ruthenium atom in question. *, $\alpha = 1$; C(2)–Ru(2)–C(21, 22, 200) are 98.8(2), 80.5(3), 121.9 (**2a**); 97.2(4), 79.3(4), 126.2 (**2b**); 101.8(3), 81.7(3), 121.5° (**3b**); Ru(n)–C(α) is Ru(2)–C(1); Ru(2)–C(2) are 2.388(5) (**2a**), 2.42(1) (**2b**), 2.509(6) Å (**3b**).

[a] For Ru(n)–C(α)–C(β) read Ru(2)–C(1)–C(2).

[b] Gives the alternate Ru(2)–C(2)–C(1).

2.4.2. Crystal and refinement data

Compound **2b**. $C_{26}H_{21}BF_4O_6Ru_3$, $M = 819.5$, space group $P\bar{1}$(No. 2), $a = 9.448(1)$, $b = 10.278(1)$, $c = 15.302(2)$ Å, $\alpha = 101.034(2)$, $\beta = 104.171(2)$, $\gamma = 92.041(2)$, $V = 1409$ Å^3; $D_{calc} = 1.93_2$ g cm^{-3} ($Z = 4$), $\mu = 16.5$ cm^{-1}. Crystal size: $0.45 \times 0.28 \times 0.04$ mm; '$T_{min/max}$' (K) = 0.75, $R = 0.051$, $R_w = 0.051$. $|\Delta\rho_{max}| =$ 0.96(4) e Å^{-3}.

Compound **3b**. $C_{18}H_{15}BF_4O_4Ru_2$, $M = 584.3$, space group $P\bar{1}$, $a = 14.265(3)$, $b = 10.454(3)$, $c = 7.299(4)$ Å, $\alpha = 98.37(5)$, $\beta = 92.57(4)$, $\gamma = 106.04(2)$, $V = 1031$ Å^3, $D_{calc} = 1.88_2$ g cm^{-3} ($Z = 4$). $\mu = 15.2$ cm^{-1}; Crystal size: $0.35 \times 0.27 \times 1.0$ mm; '$T_{min/max}$' (K) = 0.90, $R =$ 0.055, $R_w = 0.057$. $|\Delta\rho_{max}| = 1.36$ (9) e Å^{-3}.

Table 2
Bond lengths (Å) and angles (°) for the metal–carbide interactions

Compound	**2a** [4]	**2b**	**3b**
Bond lengths			
Ru(2)–C(1)	2.324(5)	2.32(1)	2.224(7)
Ru(2)–C(2)	2.388(5)	2.42(1)	2.509(6)
Ru(3)–C(2)	2.044(6)	2.06(1)	2.023(5)
X–C(1)	2.065(6)	2.07(1)	0.99
C(1)–C(2)	1.222(9)	1.22(2)	1.213(8)
Bond angles			
Ru(2)–C(1)–X	129.5(3)	130.8(5)	122.7(4)
Ru(2)–C(2)–Ru(3)	132.7(3)	132.9(5)	132.7(3)
Ru(3)–C(2)–C(1)	155.2(3)	156.7(8)	164.7(5)
X–C(1)–C(2)	152.5(4)	149.3(8)	148.0(7)

3. Results and discussion

3.1. Protonation of [{Ru(CO)$_2$(η-C$_5$H$_4$R)}$_2$(μ$_2$-C≡C)] (R = H, **1a**; Me, **1b**)

We have already reported the synthesis of **2a** by an easily reproducible route and described its remarkable fluxional motion exchanging all three ruthenium atoms [4]. However, we first encountered this complex from the treatment of complex **1a** with $HBF_4 \cdot Et_2O$ at ambient temperature in diethyl ether which gave an immediate precipitate (Scheme 1). Akita has reported that the analogous iron ethynediyl underwent a straightforward protonation giving a monocation, [{Fe(CO)$_2$(η-C$_5$Me$_5$)}$_2$(μ$_2$-η^1:η^2-C≡CH)](BF$_4$) (**4**). Subsequently, the addition of $HBF_4 \cdot Et_2O$ to a diethyl ether solution of complex **1a** was performed at 0 °C giving a similar yellow precipitate again. However, the infrared spectrum of the precipitate contained three sharp ν(CO) absorptions at 2072, 2062 and 2018 cm^{-1}, differing significantly from the spectrum observed for **2a** but still indicative of a cationic complex. The FAB mass spectrum confirmed that the isolated material differed

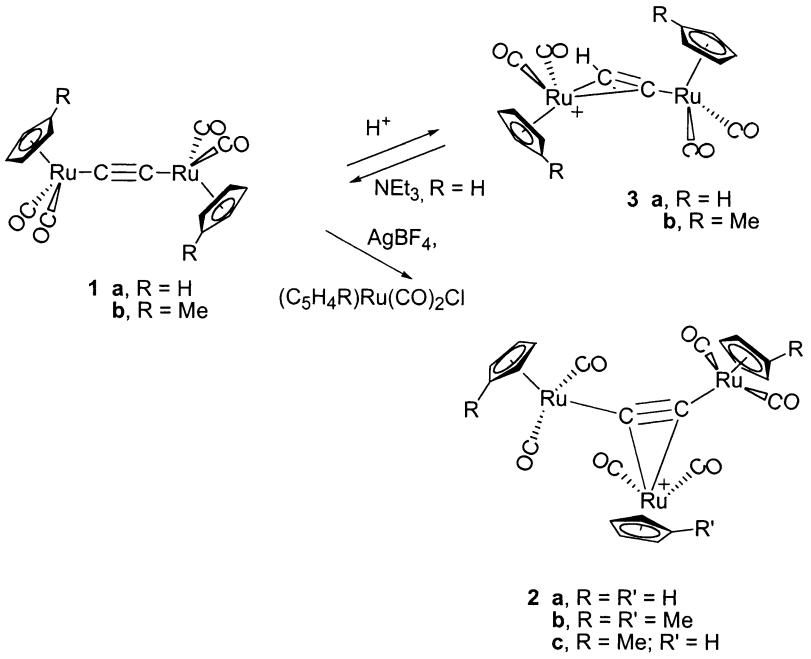

Scheme 1.

to that of **2a**, with an ion at *m*/*z* 470 assigned to $[\{Ru(CO)_2(C_5H_5)\}_2(C{\equiv}CH)]^+$. Ions at *m*/*z* 664–608 were assigned to the sequential loss of three carbonyl ligands from this ion. The ^{1}H-NMR spectrum consisted of a singlet resonance at δ 5.67 ppm assigned to Ru(η-C_5H_5), and a resonance at δ 3.86 ppm, which integrated in a ratio of 1:10. The ^{13}C-NMR spectrum contained singlet resonances at δ 196.2 and 90.3 ppm attributed to terminal carbonyl and cyclopentadienyl ligands, respectively, along with singlet resonances assigned to the carbons of an ethynyl ligand appearing at δ 88.8 (C≡C) and 75.9 ppm (C≡CH). The later resonance was broadened significantly. The preceding data was consistent with that of the cationic diiron ethynyl complex **4** and as such was assigned as $[\{Ru(CO)_2(\eta\text{-}C_5H_5)\}_2(\mu_2\text{-}\eta^1{:}\eta^2\text{-}C{\equiv}CH)](BF_4)$ (**3a**) but unfortunately crystals suitable for a X-ray structural determination of the complex were not forthcoming. In support of this assignment, **3a** was readily deprotonated with NEt_3 to quantitatively return **1a**.

Addition of $HBF_4{\cdot}x(Et_2O)$ to complex **1a** at a range of temperatures was found to yield **3a**. It should be noted that the presence of **2a** was not observed in all cases. Precisely why the protonation of complex **1a** to give **2a** was unable to be reproduced is unclear. Presumably the addition of excess $HBF_4{\cdot}x(Et_2O)$ or exposure of the sample to aerial oxidation were possible sources of contamination and so **3a** was treated independently with those reagents, respectively, and the reactions monitored by infrared spectroscopy. Absorptions attributable to **3a** are observed throughout both reactions while several unidentified absorptions appear in each reaction indicating a mixture of products. Attempts at separating the resultant mixtures were unsuccessful but, importantly, absorptions attributable to **2a** were not observed. The protonation of $[\{Re(CO)_5\}_2(\mu_2\text{-}C{\equiv}C)]$ with HCl or $HOSO_2F$ was reported by Beck and co-workers to yield HC≡CH and $[Re(CO)_5X]$ (X = Cl, OSO_2F) [14]. Speculation regarding the mechanism of this reaction was absent from this paper but with this report in mind, the possible formation of complex **2a** has been rationalised as protonation of the C_2^{2-} anion, affording HC≡CH and $\{Ru(OEt_2)(CO)_2(\eta\text{-}C_5H_5)\}$ with this cation then being coordinated by another equivalent of **1a** to give **2a** (Equation 1).

$$3[\{Ru(CO)_2(\eta C_5H_5)\}_2(\mu_2 C{\equiv}C)]\ (\mathbf{1a}) + 2HBF_4 \cdot x(Et_2O) \rightarrow 2[\{Ru(CO)_2(\eta C_5H_5)\}_2(\mu_3 C{\equiv}C)](BF_4)\ (\mathbf{2a}) + HC{\equiv}CH_{(g)} + xEt_2O \quad (1)$$

Treatment of complex **1b** with $HBF_4{\cdot}Et_2O$ at ambient temperature leads to an immediate yellow precipitate, which upon recrystallisation from CH_2Cl_2–Et_2O, gave a specimen suitable for a single-crystal X-ray structural determination, being identified as $[\{Ru(CO)_2(\eta\text{-}C_5H_4Me)\}_2(\mu_2\text{-}\eta^1{:}\eta^2\text{-}C{\equiv}CH)](BF_4)$ (**3b**), with no spectroscopic evidence found for the presence of **2b**.

The infrared spectrum of **3b** contains three ν(CO) absorptions which differ by only $\sim$2 cm^{-1} to those observed for **3a**. The FAB mass spectrum consists of a base peak corresponding to $[M]^+$ at *m*/*z* 498 with ions indicative of sequential loss of three carbonyl ligands. The ^{1}H-NMR spectrum consists of four singlet resonances at δ 5.03, 5.01, 4.97 and 4.95 ppm assigned to

Ru(η-C_5H_4Me) and a singlet resonance at δ 1.57 ppm assigned to the methyl protons of the same ligand. The resonance observed at δ 3.83 ppm is attributed to the proton of the ethynyl ligand and comparing well to that of complexes **4** [10] and **3a**. The ^{13}C-NMR spectrum contained resonances for the substituted cyclopentadienyl and terminal carbonyl ligands at the expected chemical shifts. Resonances assigned to the carbons of the alkynyl ligand appear at δ 89.4 (C≡C) and 80.0 ppm (≡CH), with the latter singlet broadened in a similar manner to that of **3a**.

3.2. Silver halide precipitation reactions

Our earlier report of the silver cation route [4] to complexes **2** appears to be general with the ability to form a Ag^+ complex of the requisite ethyne-1,2-diyl being the determining factor. In fact we have now found that the formation of **2a** is best undertaken by the in-situ reaction of **1a** with [$RuCl(CO)_2(\eta$-$C_5H_5)$] (**6**) in the presence of [$AgBF_4$]. An NMR experiment involving these reagents showed after 12 h a mixture of the trisilver ethyne-1,2-diyl complex [$Ag_3(\{Ru(CO)_2(\eta$-$C_5H_5)\}_2(\mu_2$-C≡C)$\}_3](BF_4)_3$, **2a**, **1a**, and **6** which were identified by their characteristic (η-C_5H_5) resonances. After 32 h the reaction appeared complete although the spectra showed that a cationic impurity was present.

Extension of this methodology to the synthesis of [$\{Ru(CO)_2\{\eta$-$C_5H_4Me)\}_3(\mu_3$-C≡C$\}](BF_4)$ (**2b**) and [$\{Ru(CO)_2(\eta$-$C_5H_5)\}\{Ru(CO)_2(\eta$-$C_5H_4Me)\}_2(\mu_3$-C≡C)$](BF_4)$ (**2c**) has also proved successful. The spectroscopic properties of **2b** and **2c** differ only in the expected ways from those of **2a** [4] given that these complexes contain methyl substituted cyclopentadienyl groups. The infrared spectra of **2b**,**c** contain three strong ν(CO) absorptions between 2055 and 1992 cm^{-1} and are comparable to that of **2a**. The FAB mass spectra also closely resemble that of **2a** with a base peak in each corresponding to $[M-(BF_4)]^+$ and ions corresponding to successive loss of three carbonyl ligands. The ^{1}H-NMR spectra of **2b**,**c** contain singlet resonances at δ 2.09 and 2.06 ppm, respectively, attributed to Ru(η-C_5H_4*Me*). The resonances attributed to the methine protons are observed as two apparent triplets of second-order AA′:BB′ spin systems centred at δ 5.70 and 5.61 ppm for **2b** and δ 5.70 and 5.60 ppm for **2c**. Additionally, the spectrum of **2c** contains a singlet resonance at δ 5.81 ppm assigned to Ru(η-C_5*H*$_5$). The ^{13}C-NMR spectrum of each complex is uncomplicated with resonances at expected chemical shifts for the substituted and unsubstituted cyclopentadienyl ring carbons and carbonyl ligands. A resonance attributable to the acetylenic carbons of the complexes was not observed. A similar fluctional process that served to exchange the three {$Ru(CO)_2(\eta$-$C_5H_5)$} environments of **2a** was suspected to also be in play for **2b**. However, in order to confirm this, the solution state structure was probed by a variable temperature ^{1}H-NMR experiment over the range 24 to −70 °C. The experiment was undertaken in d_6-acetone over the range 21 to −90 °C without incident and the results were similar to those of found for **2a** insofar as lowering of the sample temperature showed minimal effect on the acquired spectra with the continued observation of resonances of the AA′:BB′ spin system and methyl proton of the C_5H_4Me ligands. Thus the previously proposed mechanism for exchange observed in the spectra of **2a** [4] seems to be in operation in the spectra of **2b**.

3.3. Solid state structures of [$\{Ru(CO)_2(\eta$-$C_5H_4Me)\}_3(\mu_3$-C≡C$)](BF_4)$ (**2b**) and [$\{Ru(CO)_2(\eta$-$C_5H_4Me)\}_2(\mu_2$-η^1:η^2-C≡CH$)](BF_4)$ (**3b**)

The complexes crystallise in the centrosymmetric space group $P\bar{1}$ with two complete cations and two tetrafluoroborate anions in the unit cell. The molecular structures of **2b** and **3b** are shown in Fig. 1, together with the numbering schemes used; pertinent bond lengths and angles are presented in Tables 1 and 2. The cation of **2b** is devoid of any intrinsic symmetry and, in a manner similar to the solid state structure of **2a**, three {$Ru(CO)_2(\eta$-$C_5H_4Me)$} groups surround a C≡C unit with two of the three metal fragments bound in η^1 fashion and the remaining fragment (Ru(2)) bound in an essentially symmetrical η^2 fashion. The three ruthenium atoms and acetylenic carbons are co-planar with the sum of the angles about C(1) and C(2) each equal to 360°. The measured Ru–C(sp) bond lengths are 2.07(1) Å (Ru(1)–C(1)) and 2.06(1) Å (Ru(3)–C(2)), with distances for the π-bound metal fragment of 2.32(1) and 2.42(1) Å for Ru(2)–C(1) and Ru(2)–C(2), respectively. The geometry about each of the ruthenium centres is unremarkable and there is no discernable difference between the neutral and cationic ruthenium centres. The measured C(1)–C(2) distance of 1.22(2) Å is identical to that observed in the solid state structure of **2a** and suggests that for both complexes, substantial triple bond character remains upon metal coordination. Rotation about the Ru(3)–C(sp) bond results in the cyclopentadienyl ligand coordinated to Ru(3) being orientated in an anticlinal fashion to those coordinated to Ru(1) and Ru(2) which lie in a similar arrangement to that observed for **2a**. As proposed for **2a**, this orientation presumably serves to accommodate the steric bulk of the {$Ru(CO)_2(\eta$-$C_5H_4Me)$} groups about the C≡C unit. The cations of **3b** present in the asymmetric unit are identical comprising an ethynyl moiety σ-bonded to a {$Ru(CO)_2(C_5H_4Me)$} group (Ru(2)) with distorted η^2 coordination to a second {$Ru(CO)_2(C_5H_4Me)$} group (Ru(1)). The hydrogen atom of the ethynyl moiety was located in the electron density difference map and constrained at a fixed position in the refinement. As

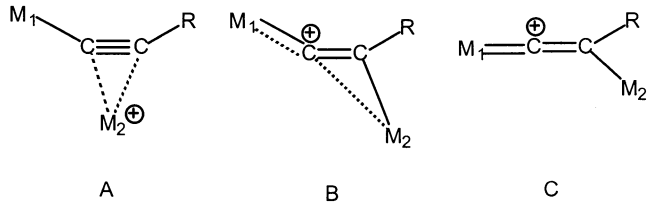

Fig. 2. Extreme conformations of putative vinylidene structures of **4** and **5**.

observed in the solid state structure of the cationic triruthenium complex **2a** [4] there are no discernable differences in geometry about the neutral and cationic ruthenium centres; overall the structure is comparable to the cationic ethynyl complexes of the similar literature precedents **4** [15] and **5**.

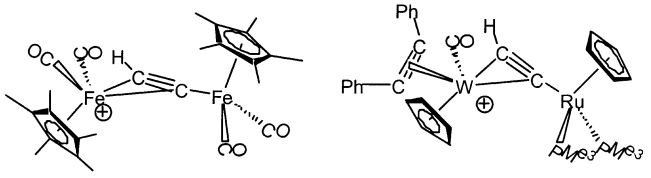

4 **5**

Selegue and Akita both presented a number of limiting structures for $[M_1M_2(\mu_2\text{-}C_2R)]^+$ complexes in their examination of the molecular structures of **4** and **5**, respectively (Fig. 2). Influence of the vinylidene limiting structure (C) was proposed as the reason for the distorted metal-(η^2-C_2H) coordination in both complexes, such that M_2 lies significantly closer to C(2) than C(1) with a decrease in the M_1–C(1) bond length.

Similar observations can be made for **3b** (Table 2) where the measured Ru(2)–C(1) and Ru(2)–C(2) distances are 2.234(7) and 2.509(5) Å, respectively, with the Ru(2)–C(sp) bond length of 2.023(5) Å slightly shorter from that in **1b**. The C(1)–C(2) distance measured for the ethynyl bridge (1.213(8) Å) is not significantly elongated from that of **1b** (1.205(9) Å), suggesting the vinylidene limiting structure is not the primary contributor to the observed structure. The Ru(2)–C(2)–C(1) vector deviates significantly from linearity (164.7(5)°), as expected, given coordination of the ethynyl ligand to the {Ru(2)$(CO)_2$(η-C_5H_4Me)} fragment.

4. Conclusion

It is clear that the protonation reaction that lead to the formation of complex **2a** was serendipitous and that our attempts to reproduce that chemistry have been unsuccessful. However, the subsequent protonation of ethynediyl complexes has given the expected μ-ethynyl complex, which could be deprotonated. The novel Ru_3C_2 complexes **2** are best produced from the silver halide precipitation reaction we have described previously [4].

5. Supplementary material

Crystallographic data for the structural analyses have been deposited with the Cambridge Crystallographic Data Centre, CCDC Nos. 197291–2. Copies of this information may be obtained free of charge from The Director, CCDC, 12 Union Road, Cambridge CB2 1EZ, UK (fax: +44-1223-336033; e-mail: deposit@ccdc.cam.ac.uk; or www: http://www.ccdc.cam.ac.uk).

Acknowledgements

C.S.G. was the holder of a Australian Postgraduate Award.

References

[1] C.S. Griffith, G.A. Koutsantonis, B.W. Skelton, A.H. White, Chem. Commun. (1998) 1805.
[2] L.T. Byrne, C.S. Griffith, G.A. Koutsantonis, B.W. Skelton, A.H. White, J. Chem. Soc. Dalton Trans. (1998) 1575.
[3] L.T. Byrne, C.S. Griffith, J.P. Hos, G.A. Koutsantonis, B.W. Skelton, A.H. White, J. Organomet. Chem. 565 (1998) 259.
[4] C.S. Griffith, G.A. Koutsantonis, B.W. Skelton, A.H. White, Chem. Commun. (2002) 2174.
[5] L.T. Byrne, J.P. Hos, G.A. Koutsantonis, B.W. Skelton, A.H. White, J. Organomet. Chem. 592 (1999) 95.
[6] L.T. Byrne, J.P. Hos, G.A. Koutsantonis, B.W. Skelton, A.H. White, J. Organomet. Chem. 598 (2000) 28.
[7] M.I. Bruce, Chem. Rev. 98 (1998) 2797.
[8] M.I. Bruce, A.G. Swincer, Adv. Organomet. Chem. 22 (1983) 59.
[9] N.M. Kostic, R.F. Fenske, Organometallics 1 (1982) 974.
[10] M. Akita, M. Terada, S. Oyama, Y. Moro-oka, Organometallics 9 (1990) 816.
[11] M. Akita, Y. Moro-oka, Bull. Chem. Soc. Jpn. 68 (1995) 420.
[12] G.A. Koutsantonis, J.P. Selegue, J. Am. Chem. Soc. 113 (1991) 2316.
[13] S.R. Hall, G.S.D. King, J.M. Stewart (Eds.), The XTAL 3.5 System, University of Western Australia, 1996.
[14] M. Appel, J. Heidrich, W. Beck, Chem. Ber. 120 (1987) 1087.
[15] K.G. Frank, J.P. Selegue, J. Am. Chem. Soc. 112 (1990) 6414.